2015-05

Integrated range-Doppler map and extended target identification with adaptive waveform for cognitive radar

Romero, Ric A.

IEEE

Integrated range-Doppler map and extended target identification with adaptive waveform for cognitive radar

Jo-Yen Nieh, Ric A. Romero
Department of Electrical and Computer Engineering
Naval Postgraduate School
Monterey, CA, USA
{jnieh,rnromero}@nps.edu

***Abstract*—In this paper, we propose an integrated scheme to identify an extended moving target while trying to correctly locate its peak range-Doppler cell. The scheme is extended to handle multiple target responses. The cognitive radar platform uses adaptive waveform based on the eigenwaveform. Two real-time adaptive waveforms called maximum a posteriori probability weighted eigenwaveform (MAP-PWE) and match-filtered PWE (MF-PWE) are combined with range-Doppler map (RDM) technique to execute target type identification for moving extended targets. Joint RDM cell localization and target identification performance comparison between a traditional pulsed wideband waveform, MAP-PWE, and MF-PWE techniques are shown. It is noted the MF-PWE performs better than the wideband and MAP-PWE.**

Keywords—adaptive waveform design, range Doppler map, identification, eigenwaveform, cognitive radar

I. INTRODUCTION

A good and common model in radar is to assume that the targets are point targets. Our interest, however, is extended target and matched illumination [1-3]. The SNR-based waveform matched to a known extended target is sometimes referred to as the eigenwaveform. Target identification applications with adaptive waveforms in a cognitive radar platform are tackled in [4-6]. In [7], the authors proposed the problem of identifying a moving extended target while trying to locate its range-Doppler location, i.e., the target RDM cell with the largest return. In this paper, we extend the problem for multiple moving extended targets. In [4], it has been shown that eigenwaveform based waveforms seem to perform better than most waveforms considered for static target recognition problem. Combining range-Doppler map technique with the the PWE-based adaptive waveform, we propose a scheme that is capable of extended target recognition while correctly locating range-Doppler cells for multiple moving targets. Joint performance in terms of identification and correctly locating RDM cell between wideband, MAP-PWE, and MF-PWE techniques are shown.

II. EIGENWAVEFORM AND TARGET IDENTIFICATION SCHEME

The goal of this work is to produce an integrated scheme using eigenwaveform-based adaptive waveforms to perform target classification and range-Doppler location for multiple moving extended targets. In this section, we give a quick review of the optimum transmit waveform matched to an extended target and the probability weighted eigenwaveform (PWE) that is used for target recognition with a cognitive radar platform.

A. Optimum Transmit Waveform for Extended Target

Let $\mathbf{h}$ be a discrete target response, $\mathbf{x}$ be a transmit signal, and let the $\mathbf{s}$ be their convolution response. The largest peak of matched filter is achieved by utilizing the eigenvector $\mathbf{q}_{\max}$ (referred to as eigenwaveform throughout the paper) corresponding to the largest eigenvalue $\lambda_{\max}$ from the auto-correlation matrix of target response as the transmit signal $\mathbf{x}$. The target autocorrelation matrix is given by

$$\mathbf{R}_h = \mathbf{H}^H\mathbf{H}$$

where $\mathbf{H}$ is the convolution matrix given by

$$\mathbf{H} = \begin{bmatrix} \mathbf{h} & 0 & 0 & 0 \\ . & \mathbf{h} & 0 & 0 \\ . & . & .. & .. \\ . & & & \mathbf{h} \end{bmatrix}.$$

The energy of $\mathbf{s}$ is clearly given by

$$E_s = \mathbf{x}^H\mathbf{H}^H\mathbf{H}\mathbf{x} = \mathbf{x}^H\mathbf{R}_\mathbf{H}\mathbf{x}. \quad (1)$$

Thus, the maximum energy of (1) using eigenwaveform as the transmit signal is given by

$$E_{s_{max}} = \mathbf{x}^H\mathbf{R}_\mathbf{H}\mathbf{x} = {\mathbf{q}_{\max}}^H\lambda_{\max}\mathbf{q}_{\max} = \lambda_{\max}E_x. \quad (2)$$

where E_x is the energy of transmit signal $\mathbf{x}$.

B. Targets Identification with MAP-PWE

The MAP-PWE approach using adaptive waveform design was first introduced in [4] inspired by other very effective approaches in [2, 4-5]. By using likelihood based metric from probability density function as weights via multiple hypothesis testing, MAP-PWE adaptive waveform seemed to be the best performer in terms of target recognition (among previous approaches). As such we will utilize it here. Moreover, we introduce a simpler version of MAP-PWE called (matched filter) MF-PWE which turned out to perform even better than MAP-PWE. We compare both against a benchmark pulsed wideband waveform. These waveforms are used in a target

recognition CR platform first introduced by Goodman, et al in [5]. We now quickly review the CR platform and how MAP-PWE adaptive waveform is produced.

Consider a target identification problem in which one of M possible targets is present. Each target hypothesis is characterized by its impulse response $\mathbf{h}_j, j = 1, 2, ...M$ which is assumed a priori. Assuming all targets are of length N and there is one target present, the detection hypotheses are

$$\begin{aligned} H_1 &: \mathbf{y} = \mathbf{x} * \mathbf{h}_1 + \mathbf{w} = \mathbf{H}_1\mathbf{x} + \mathbf{w} \\ H_2 &: \mathbf{y} = \mathbf{x} * \mathbf{h}_2 + \mathbf{w} = \mathbf{H}_2\mathbf{x} + \mathbf{w} \\ &.. \\ H_M &: \mathbf{y} = \mathbf{x} * \mathbf{h}_M + \mathbf{w} = \mathbf{H}_M\mathbf{x} + \mathbf{w} \end{aligned}$$

where the $\mathbf{H}_j$ is the convolution matrix of target j and $\mathbf{w}$ is the complex-valued AWGN with a sample variance of σ^2. For brevity in succeeding equations, let's assume σ to be one.

In PWE, the transmit signal is the sum combination of each unit energy eigenvector $\mathbf{q}_j$ each weighted by $\sqrt{w_j}$ where w_j is the weight distribution for the j^{th} hypothesis calculated from prior received signal. The energy constraint of transmit signal E_x in the end actually dictates the energy weight distribution of each eigenwaveform. However, to simplify the procedure it is best to simply add the weights to sum up to 1 (as an intermediate normalization step). In other words,

$$\sum_{j=1}^{M} w_j = 1, \tag{3}$$

and

$$\bar{\mathbf{x}} = (\sum_{j=1}^{M} \sqrt{w_j}\mathbf{q}_j) \tag{4}$$

where $\bar{\mathbf{x}}$ is the direct combination result of all eigenvector $\mathbf{q}_j$. However, $\bar{\mathbf{x}}$ may not be unit-energy after summation since the eigenwaveforms themselves come from different targets and may not be orthogonal. Although the energy may be close to 1, it still needs to be normalized such that the energy constraint can easily be factored in i.e.,

$$\mathbf{x} = \sqrt{E_x}\frac{\bar{\mathbf{x}}}{\sqrt{E_{\bar{x}}}}. \tag{5}$$

Now, we discuss how the waveform weights are calculated. Let $f_{j|i}(\mathbf{y})$ be the probability density or likelihood function of the j^{th} hypothesis given i^{th} target is the present target assuming additive white Gaussian noise where we assumed $\sigma = 1$ to simplify our equations. The probability density or likelihood function is given by

$$\begin{aligned} f_{j|i}(\mathbf{y}) &= \beta \exp[-(\mathbf{y} - \mathbf{s}_j)^H(\mathbf{y} - \mathbf{s}_j)] \\ &= \beta \exp[-\mathbf{y}^H\mathbf{y} + \mathbf{y}^H\mathbf{s}_j + {\mathbf{s}_j}^H\mathbf{y} - {\mathbf{s}_j}^H\mathbf{s}_j] \\ &= \beta \exp[-\mathbf{y}^H\mathbf{y} + 2\,\mathrm{Re}({\mathbf{s}_j}^H\mathbf{y}) - {\mathbf{s}_j}^H\mathbf{s}_j] \end{aligned} \tag{6}$$

where

$$\beta = \frac{1}{\pi^n}$$

is the constant in front of the Gaussian distribution. Let w_j^1 be the initial waveform weight for each hypothesis as dictated by (4). If there is no a priori information available as to the likelihood of each hypothesis, then initially we can assume them to be equally likely i.e., $w_j^1 = 1/M$. Let $f_j^P(\mathbf{y})$ be the likelihood function from P^{th} return signal, then the waveform weights w_j^{P+1} are updated by the likelihood values from the latest P^{th} return signal. In other words, for multiple illumination the waveform weights are updated as

$$\begin{aligned} w_i^1 &= \frac{1}{M} \\ w_i^2 &= \alpha^1 w_i^1 f_i^1 \\ w_i^3 &= \alpha^2 w_i^2 f_i^2 \\ &... \\ w_i^{P+1} &= \alpha^P w_i^P f_i^P \end{aligned} \tag{7}$$

where f_j^P is the calculated likelihood value after P^{th} transmission and the weight w_j^{P+1} is the weight distribution corresponding to the j^{th} hypothesis for the $(P+1)^{th}$ transmission (or P updates) while α^P ensures unity weight summation as dictated by (3) in each transmission. In other words, w_j^{P+1} is the waveform weight of j^{th} eigenwaveform in (4).

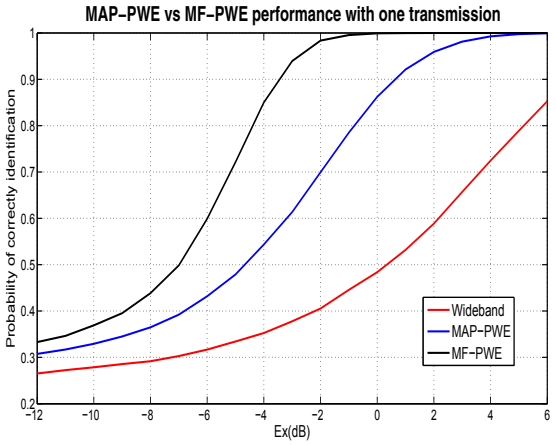

Fig. 1. Performance comparison: Wideband, MAP-PWE and MF-PWE with one transmission.

C. Target Identification with MF-PWE

The MF-PWE is first proposed in [7] where the constant and biased terms in (6) are removed to improve performance. In other words, it proposed $f_{j|i}(\mathbf{y})$ to be of the form

$$f_{j|i}(\mathbf{y}) = \beta \exp[2\,\mathrm{Re}(\mathbf{s}_j^H\mathbf{y})] \tag{8}$$

where β now here is a constant that ensures the waveform weights sum up to one as dictated by (3). Now, it is clear in (8) that the biased terms where MAP is used in (6) would be removed. Lastly, the waveform weight update rule remains the same for MF-PWE as dictated in (7).

The performance comparisons between a non-adaptive pulsed wideband waveform, MAP-PWE and MF-PWE vs various number of transmissions are shown in Fig. 1 and Fig. 2 via Monte Carlo simulations. When the number of transmissions is fixed, the hypothesis with the largest updated waveform weight is decided to be the correct hypothesis (whether true or not). It is clear in Fig. 1 that MF-PWE has the better identification performance than MAP-PWE even with one transmission. In

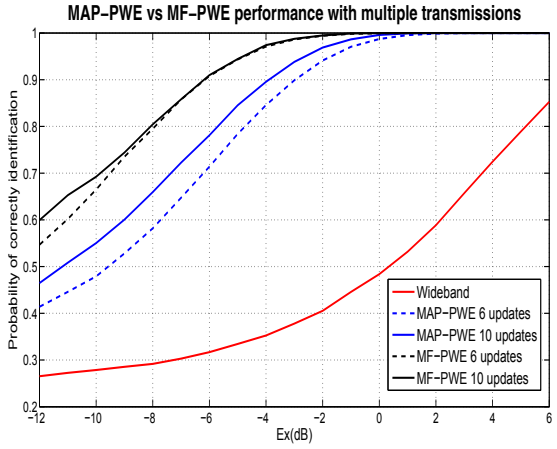

Fig. 2. Performance comparison: Wideband, MAP-PWE and MF-PWE with multiple transmissions.

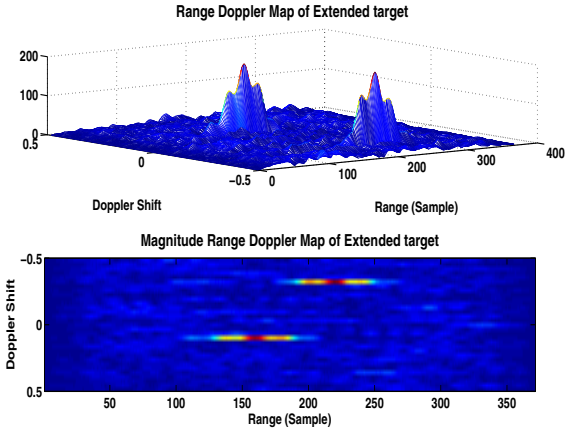

Fig. 3. Range Doppler map of two targets of the same type (some noise added).

other words, the radar is not even closed-loop in that scenario. Both PWE-based adaptive waveforms performed better than a non-adaptive wideband waveform for multiple transmissions as shown in Fig. 2.

In conclusion, MF-PWE performs better than MAP-PWE as a CR adaptive waveform in terms of target identification. Moreover, it is more computationally efficient than MAP-PWE.

III. Integrated Detection and Identification Scheme for Moving Targets

A simple integrated scheme for a single moving target identification and range-Doppler peak cell localization is proposed in [7]. It is our goal to expand and simultaneously identify multiple target types, determine how many targets in each type and correctly locate the ranges and Doppler shifts for multiple moving targets. We investigate different scenarios and finally form our comprehensive scheme.

A. Two Target of Same Type Scenario

In this section, the goal is to jointly locate (in range and Doppler) and identify two targets of the same type with arbitrary speeds and delays (range). In Fig. 3 we illustrate the two present extended targets in range-Doppler map (RDM) where a small amount of noise is added. The top panel is a three-dimensional RDM. The bottom panel is a two-dimensional RDM (which is the conventional way of illustrating RDM). The overall probability of correctly locating extended targets in range-and-Doppler and identifying target type is clearly a function of received signal-to-noise ratio, number of transmissions L, the PWE scheme chosen, and the target responses themselves via maximum target eigenvalues.

For illustration, we assume $M = 4$ possible extended targets (here we call them types for the purposes of identification). Then we form the normalized eigenwaveform for each target hypothesis and scale each eigenwaveform with the square-root of the initial waveform weight assigned to each target and then form the first PWE-based waveform. Here we now send a series of pulses R times (in this work, R is 31), since we are interested in forming RDMs. For the received return from every set of R pulses, M matched filters are applied to form M RDMs. For fair comparison, we set unity energy in R pulses. Assuming N is the length of target impulse response, the matched filtered sequence takes on a length of $4N - 3$ for any target present. If the SNR is sufficient, the two highest magnitudes in the RDM may indicate the range-Doppler locations of the two targets. We pick the $4N - 3$ sequence of highest peak and use it for likelihood update calculations. We choose the target type with the largest likelihood value and pick the two range-Doppler cells with the largest magnitudes for range-Doppler peak locations. Thus, we have jointly decided the target type and the two range-Doppler locations. The illustration of RDMs updates for each target type is shown in Fig. 4 where the two targets can be easily determined in the "decided" RDM after five updates. Here, we use MF-PWE as the designated PWE scheme.

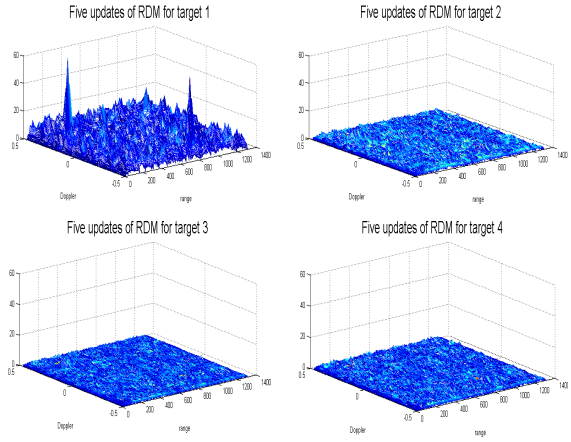

Fig. 4. Four candidate RDMs for four possible target types (where two targets of the same type are present) with PWE after six transmissions (five updates).

In Fig. 5, the probability of identification (P_i which is the probability of correctly determining target type), P_d which is the probability of correctly determining the range-Doppler location, and the overall or joint probability (P_g) with one

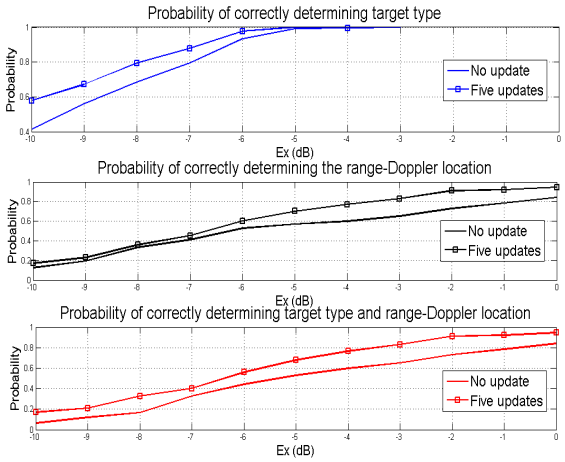

Fig. 5. Probability of correctly determining target type, probability of correctly determining the range-Doppler location, and the overall performance of correctly determining target type and range-Doppler location using MF-PWE with two targets of same type.

transmission (no update) and six transmissions (five updates) using MF-PWE scheme are shown via MC experiments. The overall probability is the probability that the range-Doppler location and target type are both correct. Notice also that the probability of correct identification is better than the probability of correctly determining the range-Doppler locations. This is because in our experiment, there are only four possible target types while there are numerous range-Doppler cells. It is also clear from Fig. 5 that the overall performance (bottom panel) is jointly affected by probability of identification and probability of correctly determining the range and Doppler location (upper and middle panels).

In summary, we modified the CR platform to adapt the assumption of two targets of same type and form a platform that can correctly identify the target and correctly indicate the range-Doppler location or cell for moving extended targets.

B. Unknown Number of Targets (Of Same Type)

In this section, we do not assume the number of targets present but at least one target present in our MC experiments. If there are multiple targets, we assume they are of the same type (i.e. same target response). Here, we modify the receiver to incorporate thresholds dictated by a given false alarm. As before, the hypothesis with the largest updated waveform weight is deemed to be the true target hypothesis. The sequences containing highest magnitudes in the chosen RDM may be retrieved for target range and Doppler location. The question here is to determine how many targets there are in latest updated RDM and what is the proper threshold to be used in locating targets range and Doppler.

Before we can determine range-Doppler location, we have to consider the problem of detection for the entire range-Doppler map since we do not know the number of targets. The detection hypotheses are

$$\begin{aligned} H_0 &: \mathbf{y} = \mathbf{w} \\ H_1 &: \mathbf{y} = \mathbf{H}_i\mathbf{x} + \mathbf{w}. \end{aligned} \tag{9}$$

It can be shown that the natural log likelihood for the null hypotheses given i^{th} target is (again setting $\sigma = 1$)

$$\ln[f_{0|i}(\mathbf{y})] = \ln\beta + 2\,\mathrm{Re}(\mathbf{s}_i^H\mathbf{w}),$$

and for the hypotheses H_1, it is

$$\ln[f_{1|i}(\mathbf{y})] = \ln\beta + 2\,\mathrm{Re}(\mathbf{x}^H\mathbf{H}_i^H\mathbf{H}_i\mathbf{x}_i + \mathbf{x}^H\mathbf{H}_i^H\mathbf{w}).$$

It can be shown that the likelihood ratio threshold r for given probability of false alarm P_{FA} and AWGN of sample variance σ_w^2 (here we leave σ arbitrary such that resulting equations follow the standard detection formulas) is of the form

$$r = \sqrt{2E_s\sigma_w^2}Q^{-1}(P_{FA}) + \ln\beta. \tag{10}$$

Thus, the probability of a target being in a specific range and Doppler location for target type i is

$$\begin{aligned} P_D &= Q\{Q^{-1}(P_{FA}) + \sqrt{\frac{2E_s}{\sigma_w^2}}\} \\ &= Q\{Q^{-1}(P_{FA}) + \sqrt{\frac{2L\mathbf{x}^H\mathbf{H}_i^H\mathbf{H}_i\mathbf{x}}{\sigma_w^2}}\} \\ &= Q\{Q^{-1}(P_{FA}) + \sqrt{\frac{2L(\sum_{j=1}^{M} w_j\mathbf{q}_j)^H\,\mathbf{R}_i(\sum_{j=1}^{M} w_j\mathbf{q}_j)}{\sigma_w^2}}\}, \end{aligned} \tag{11}$$

where $\mathbf{R}_i$ is is the autocorrelation matrix of i^{th} target response.

Again we set up Monte Carlo experiments where we randomly generate the number of targets and the range-Doppler locations of those targets. In this particular experiment we generate one, two, or three targets (of the same type) while assigning range-Doppler locations (randomly) in each experiment. In our joint recognition-detection procedure, recall that we identify the targets by choosing the RDM. Again since we do not know the number of targets, we have to perform detection via threshold in the entire RDM. The threshold is based on the PFA given a target type from (10). Once targets are "detected", then we try to determine the targets' range-Doppler locations. Using MF-PWE, we calculate the strict overall probability P_g (which is correct identification, correct number of targets and correct range-Doppler locations all at the same time) as a function of transmit energy. Notice that P_g is tied to PFA (since P_d is tied to PFA). It is clear that in Fig. 6 that the threshold (calculated from probability of false alarm) and the number of updates affect overall probability.

C. Two Targets of Different Type

In this section, we make the problem a little more interesting. Here we allow different target types to be in the scene. For now, let us limit the number of targets to two. This is akin to the "two targets of the same type scenario". However, in this problem, we have two different targets. We may consider this to be a multiple hypothesis testing (MHT) problem. Unfortunately, that can become impractical. In practice when there are more possible targets and scenarios to consider (e.g. ten targets total, two targets are type 1, 2 targets are type 2, one target is type 3, etc.), then the number of hypotheses increase dramatically. Instead we will focus on how to update the waveform weights via the likelihoods corresponding to the original four hypotheses in the target recognition problem.

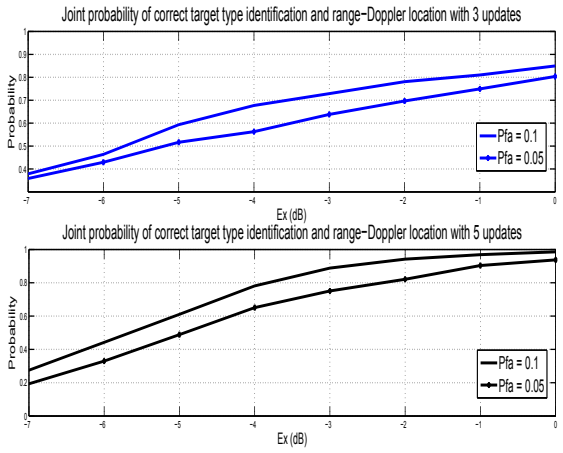

Fig. 6. Comparison of joint probability of locating correct ranges, Doppler and target types with three and five MF-PWE updates given probability of false alarm and assuming unity noise energy.

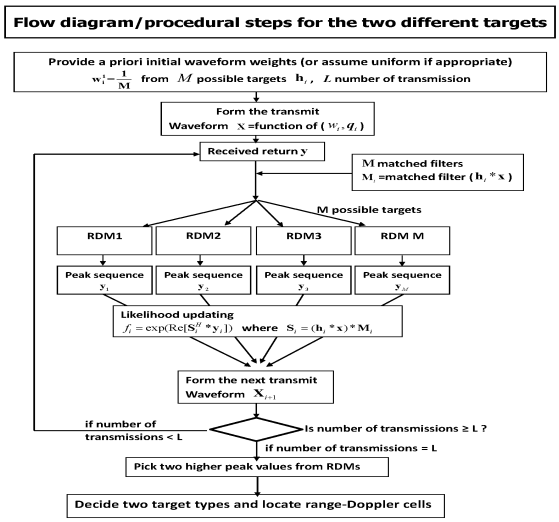

Fig. 7. Flow diagram/procedural steps for two different target types (scenario).

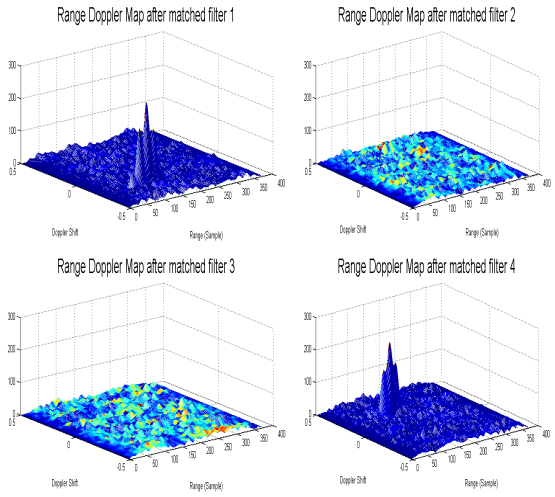

Fig. 8. Six update: RDMs of two targets from different types after M matched filters (M = 4).

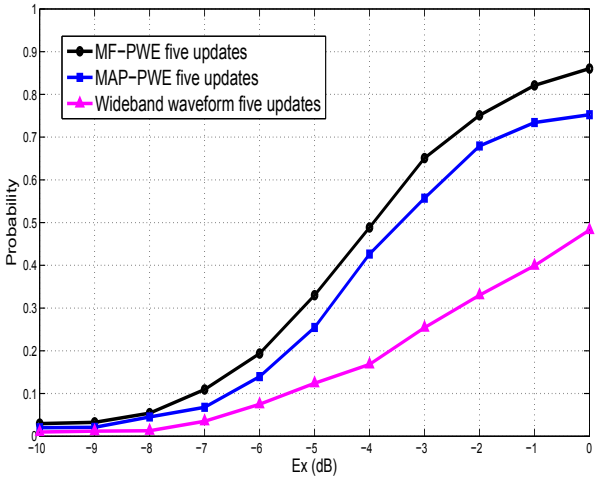

Fig. 9. Overall probability of correct target type identification and range-Doppler location for two targets of different types assuming unity noise energy.

We illustrate the procedure in Fig. 7. Interestingly, there's very little difference between this procedure to that of "two targets of the same type scenario". Here, effectively the only difference is that we choose two RDMs in the end. Also, the waveform weights will be distributed to the two target types (about 0.5 each when homing in on the two targets).

We conduct an experiment where two targets are present (type 1 and type 4) using the procedure in Fig. 7. In the four RDMs after the first transmission (no waveform update), it is difficult to tell where the targets are. Now we show what happens to the RDM after seven transmissions in Fig. 8. Notice that the two peaks in the two RDMs corresponding to targets 1 and 4.

Via Monte Carlo experiments, we illustrate the overall (or joint) probability of correctly identifying (both target present) and their range-Doppler locations in Fig. 9 with the use of MAP-PWE and MF-PWE adaptive waveforms as a function of transmit energy while varying the number or transmissions (or updates). Note here the joint performance of MF-PWE in Fig. 9 is lower than same target type scenario performance in Fig. 5. This is because the waveform weights are distributed between two targets (for different types) while the weight gets distributed mostly to one target (for same target type) which seems intuitive.

D. Unknown Number of Targets and Different Types of Targets

In this section, we assume that the number of targets is not known or there could be multiple targets of different types in the scenario. However, we assume that number of target types present is less than the possible target types. This assumption is from the intuition gained from the previous section. Our goal is to utilize the insights gained from the three scenarios above to form a comprehensive scheme to simultaneously figure out the number of targets, identify target types, and determine the range-Doppler cells of these targets.

So in this final section, we also include the case where

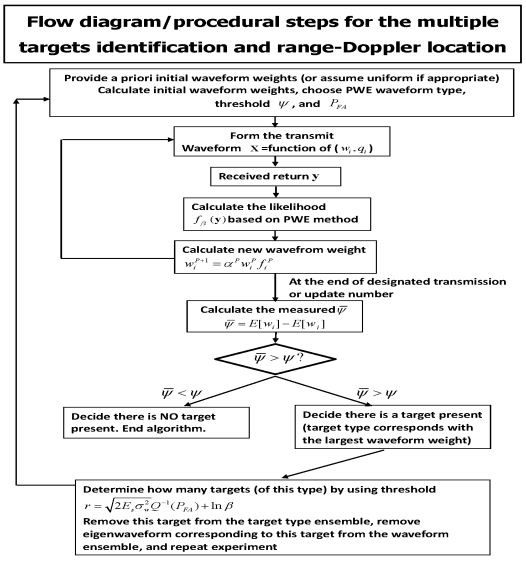

Fig. 10. Flow diagram/procedural steps of multiple targets identification and range-Doppler location algorithm.

there may not be a target. In other words, the set of algorithms in section B has to be modified to accommodate the general case when there is no target present. So here our strategy is to first figure out if there is a target or not in the scenario (after a number of transmissions/updates say L). If there is, then we figure what target type with another set of transmission (same as before i.e., L), and then another until our algorithm says there is no more target (type) present. To this end, the target identification procedure is modified by adding a user-defined threshold ψ (a percentage) and comparing that to a formulated measured $\bar{\psi}$ from the latest weight distribution. The threshold ψ as in any threshold maybe adjusted to improve decision-making of the algorithm. The smaller the threshold ψ is defined, the more sensitive or the more probable it is to identify and detect present targets.

The measured $\bar{\psi}$ is then

$$\bar{\psi} = E[w_u] - E[w_v],$$

where w_u are the weights that are above the $(100/M)$ and w_v are lower. If $\bar{\psi}$ is less than the desired ψ, then the threshold is not crossed and thus a target type is not detected. If $\bar{\psi}$ is greater than designated ψ, then we look for the target type that has the highest weight and deem that to be a present target type. Since it is deemed present, the eigenwaveform corresponding to that target is now removed from the next L number of transmissions. Now we normalize the remaining weights and try to ascertain if there are remaining targets. In other words, we terminate the transmissions when $\bar{\psi}$ is not greater than our threshold ψ. The full procedure for an experiment is summarized in Fig. 10

The overall (or joint) performance of correctly identifying the number of targets, target types, and locating range-Doppler cell for those targets is shown in Fig. 11. In this work, we use $M = 4$, $\psi = 10$, and $P_{FA} = 0.1$ to compare with various waveforms. Since our procedure identifies each target every L number of transmission (or $L-1$ updates), the plots are parameterized by number of updates per target type. It

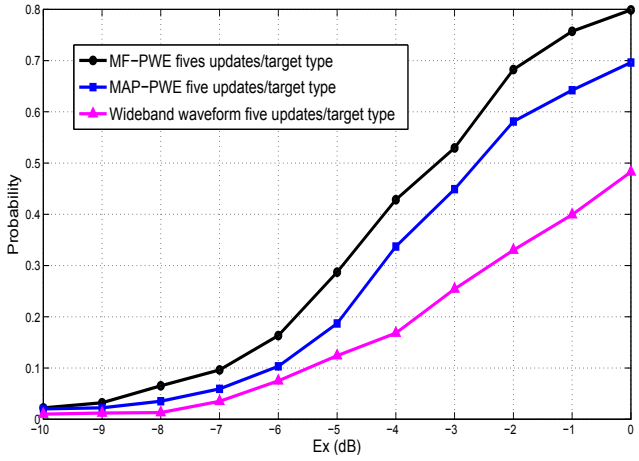

Fig. 11. Overall probability of identification and location for multiple targets of unknown types assuming unity noise energy ($\psi = 10$ percent and P_{FA} = 0.1).

is obvious that both the MAP-PWE and MF-PWE perform much better than wideband waveform as may be expected. The algorithm presented here (used in a CR platform) clearly can be used for the general problem of figuring out the number of target present, target type identification, and correctly locating range-Doppler cells of those targets.

IV. Conclusion

In this paper, an integrated scheme is proposed to perform multiple moving target types identification and range-Doppler peak cells location in cognitive radar using eigenwaveform-based adaptive waveforms for extended targets. The PWE-based waveforms are combined with range-Doppler map techniques to perform target type identification and range-Doppler cell localization for moving targets. The overall performance of identification and range-Doppler location for eigenwaveform is much improved than wideband waveform. Performance comparisons of MAP-PWE vs MF-PWE with various number of waveform transmissions are presented as comparison.

References

[1] M.R. Bell, "Information theory and radar waveform design," *IEEE. Trans. Information Theory.*, vol. 39, no. 5, pp. 1578-1597, Sep. 1993.

[2] R.A. Romero, J. Bae, and N.A. Goodman, "Theory and apllication of SNR and mutual information matched illumination waveforms," *IEEE Trans. Aerosapce and Electronic System.*, vol. 47, no. 2, pp. 912-927, Apr 2011.

[3] J. Nieh, and R.A. Romero, "Ambiguity function and detection probability considerations for matched waveform design, *IEEE Conference on Acoustics, Speech and Signal Processing.*, pp. 4280-4284, Apr 2013.

[4] R.A. Romero, and N.A. Goodman, "Improved waveform design for target recognition with multiple transmissions, *IEEE International Waveform Diversity and Design Conference.*, pp. 29-30, Feb 2009.

[5] N.A. Goodman, P.R. Venkata, and M.A. Neifeld, "Adaptive Waveform Design and Sequential Hypothesis Testing for Target Recognition With Active Sensors," *IEEE Journal of Selected Topics in Signal Processing.*, vol. 1, issue. 1, pp. 105-113, Jun. 2007.

[6] K.T. Kim, D.K. Seo, and H.T. Kim, "Radar target identification using one-dimensional scattering centres," *IET. Proceedings - Radar, Sonar and Navigation.*, vol. 148, issue. 5, pp. 285-296, Sep. 2001.

[7] J. Nieh, and R.A. Romero, "Adaptive waveform for integrated detection and identification of moving extended target, *Asilomar Conference on Signal, Systems and Computers.*, pp. 0000-0000, Nov 2014.